Imaging AGN using Gravitational Microlensing

Eight Years of Science with Chandra, 23-25 October 2007

Presented by George Chartas
Co-Is Gordon Garmire (Penn State), Xinyu Dai, Chris Kochanek, Nicholas Morgan (OSU)

Dissecting AGN Accretion Disks

- Direct imaging of accretion disks requires $\Delta\theta$ ~ nano-arcsec (at z ~ 1).

- Indirect methods of mapping the emission regions of AGN are :

(a) Light travel time arguments
(b) Reverberation mapping of the broad line region and Fe Ka emission regions
(c) Microlensing of the optical and X-ray continuum regions

Our study focuses on method (c).

The different changes in the image flux ratios with wavelength will constrain the relative sizes of the optical and X-ray emission regions

Optical and X-ray monitoring of microlensing events in AGN

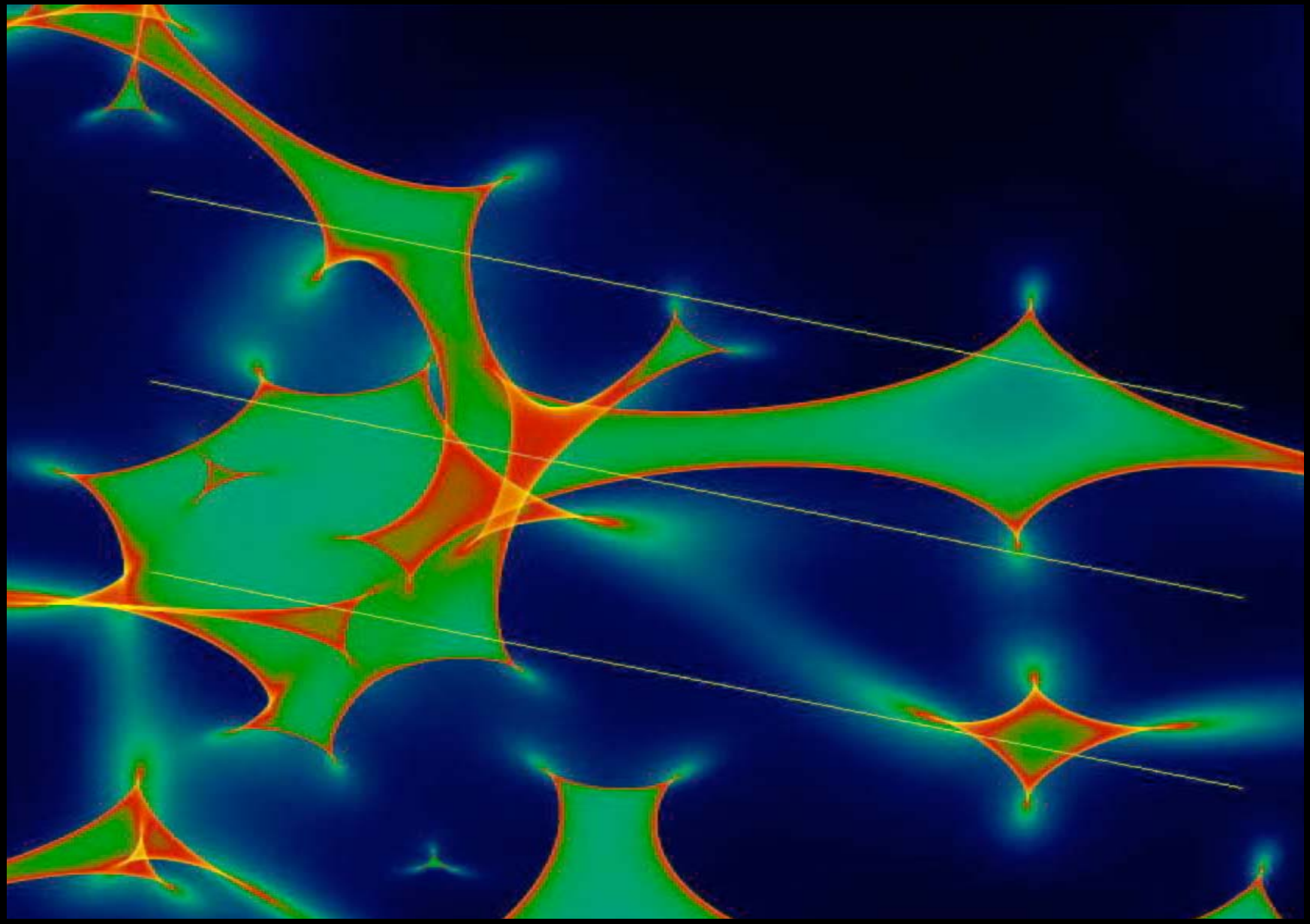

- The magnification patterns have a characteristic size scale of ζ_E called the Einstein radius (for Q1131-1231 (z_s = 0.658, z_l=0.295)):

$$\zeta_E = \sqrt{\frac{4GM_{star}}{c^2}\frac{D_{os}D_{ls}}{D_{ol}}} =$$

$$(3.8\times10^{16})\left[\frac{\langle M\rangle}{hM_{solar}}\right]^{1/2} cm$$

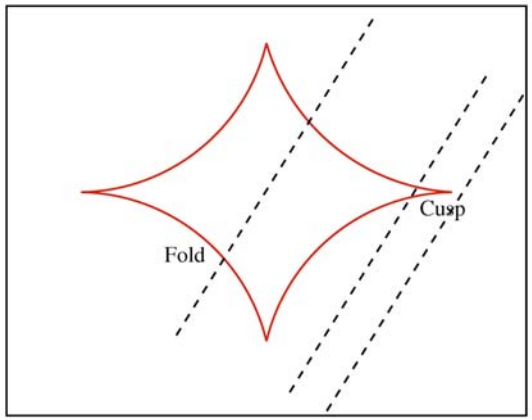

Caustic of a single star plus shear. Three tracks are shown of sources crossing fold and cusp caustics.

- Crossing time scales:

$t_E \sim \zeta_E/v_t$

$t_{HME} \sim r_s/v_t$

Optical and X-ray monitoring of microlensing events in AGN

- We have initiated a multiwavelength monitoring campaign of the quasar Q1131-1231 (z_s = 0.658, z_l=0.295) with the main scientific goal of measuring the AGN structure in the optical and X-ray bands in order to test disk models.

- X-ray monitoring observations were performed with the Chandra X-ray Observatory

- B, R and I band observations were made with the Smarts Consortium 1.2m telescope in Chile.

Optical and X-ray monitoring of microlensing events in AGN

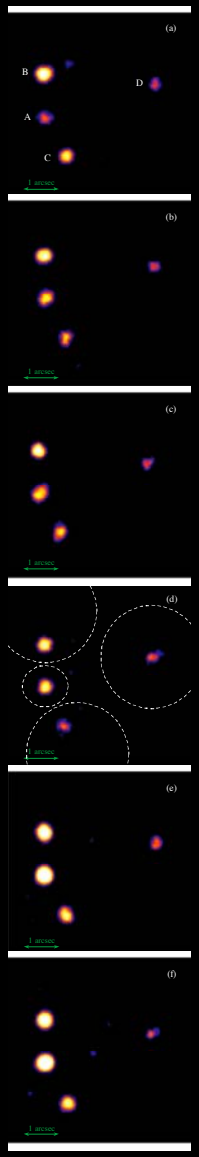

Deconvolved images in the 0.2 - 10 keV bandpass of the Chandra observations of RXJ 1131-1231.

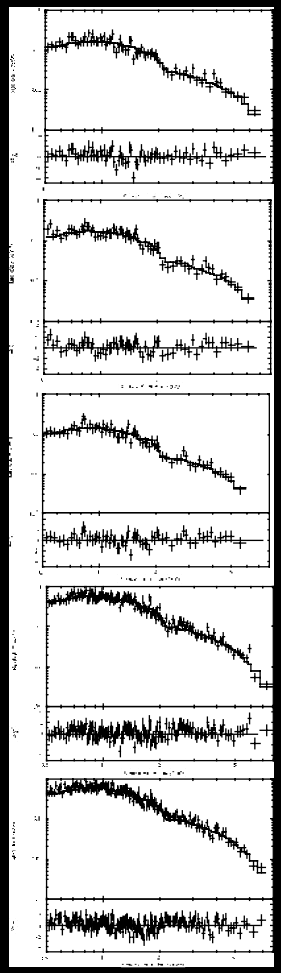

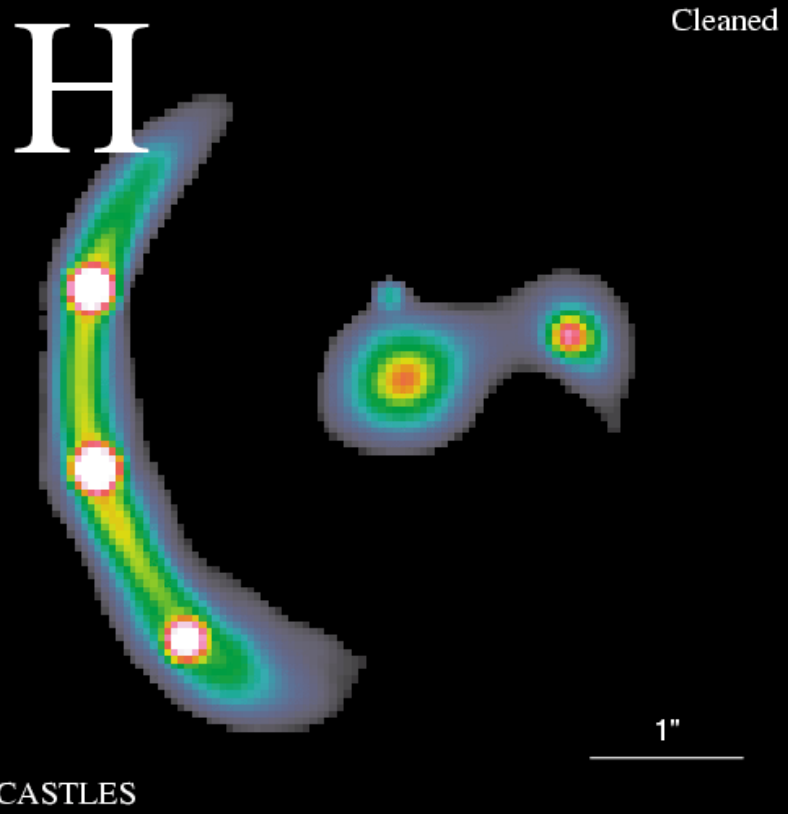

An optical image of quasar RX J1131-1231 (z_s = 0.658, z_l=0.295) taken with HST in the H-band.

Optical and X-ray monitoring of microlensing events in AGN

Observation Date	Observatory	Observation ID	Exposure Time (ks)	N_A [a]	N_B [a]	N_C [a]	N_D [a]
2004 April 12	*Chandra*	4814	10.	369 ± 19	2487 ± 50	795 ± 28	195 ± 14
2006 March 10	*Chandra*	6913	4.9	341 ± 19	619 ± 25	194 ± 14	99 ± 10
2006 March 15	*Chandra*	6912	4.4	331 ± 18	587 ± 24	222 ± 15	89 ± 9
2006 April 12	*Chandra*	6914	4.9	355 ± 19	482 ± 22	139 ± 12	128 ± 11
2006 November 10	*Chandra*	6915	4.8	3225 ± 57	1345 ± 37	349 ± 19	151. ± 12
2006 November 13	*Chandra*	6916	4.8	3333 ± 58	1541 ± 39	395 ± 20	112 ± 11

[a]Background-subtracted source counts including events with energies within the 0.2–10 keV band. The counts for images B and C for the 2004 April 12 observation are corrected for pile-up by factors of 37% and 16%, respectively. The counts for images A and B for the 2006 November 10 observation are corrected for pile-up by factor of 32% and 13%, respectively. The counts for images A and B for the 2006 November 13 observation are corrected for pile-up by factors of 33% and 17%, respectively.

Epoch	Parameter	Image A	Image B	Image C	Image D
1	Γ	$1.44^{+0.08}_{-0.08}$		$1.63^{+0.10}_{-0.10}$	$1.95^{+0.21}_{-0.20}$
	0.2–2 keV Flux (10^{-13} erg s^{-1} cm^{-2})	$0.9^{+0.1}_{-0.1}$	$6.9^{+0.6}_{-0.6}$	$2.3^{+0.4}_{-0.4}$	$0.6^{+0.2}_{-0.2}$
	$C-statistic/nbins$	556/789		599/789	368/789
2	Γ	$1.58^{+0.15}_{-0.15}$	$1.63^{+0.11}_{-0.11}$	$1.62^{+0.19}_{-0.19}$	$1.66^{+0.28}_{-0.27}$
	0.2–2 keV Flux (10^{-13} erg s^{-1} cm^{-2})	$2.4^{+0.5}_{-0.5}$	$3.6^{+0.6}_{-0.5}$	$1.2^{+0.4}_{-0.3}$	$0.6^{+0.3}_{-0.2}$
	$C-statistic/nbins$	531/840	653/840	435/840	300/840
3	Γ	$1.61^{+0.15}_{-0.15}$	$1.73^{+0.11}_{-0.11}$	$1.57^{+0.18}_{-0.18}$	$1.60^{+0.28}_{-0.28}$
	0.2–2 keV Flux (10^{-13} erg s^{-1} cm^{-2})	$2.1^{+0.5}_{-0.5}$	$3.9^{+0.7}_{-0.7}$	$1.3^{+0.4}_{-0.4}$	$0.6^{+0.2}_{-0.2}$
	$C-statistic/nbins$	521/840	555/840	425/840	292/840
4	Γ	$1.53^{+0.14}_{-0.14}$	$1.64^{+0.12}_{-0.12}$	$1.70^{+0.23}_{-0.23}$	$1.62^{+0.24}_{-0.24}$
	0.2–2 keV Flux (10^{-13} erg s^{-1} cm^{-2})	$2.1^{+0.4}_{-0.4}$	$2.8^{+0.6}_{-0.5}$	$0.9^{+0.3}_{-0.3}$	$0.8^{+0.3}_{-0.3}$
	$C-statistic/nbins$	540/840	548/840	333/840	350/840
5	Γ	$1.65^{+0.07}_{-0.07}$	$1.67^{+0.05}_{-0.05}$	$1.90^{+0.15}_{-0.15}$	$1.54^{+0.22}_{-0.22}$
	0.2–2 keV Flux (10^{-13} erg s^{-1} cm^{-2})	19^{+1}_{-1}	9^{+1}_{-1}	$2.3^{+0.5}_{-0.5}$	$0.9^{+0.2}_{-0.3}$
	$C-statistic/nbins$	771/840	797/840	502/840	402/840
6	Γ	$1.51^{+0.07}_{-0.07}$	$1.82^{+0.08}_{-0.08}$	$1.76^{+0.14}_{-0.14}$	$2.28^{+0.29}_{-0.28}$
	0.2–2 keV Flux (10^{-13} erg s^{-1} cm^{-2})	19^{+1}_{-1}	11^{+1}_{-1}	$2.4^{+0.5}_{-0.5}$	$0.9^{+0.3}_{-0.3}$
	$C-statistic/nbins$	768/840	658/840	489/840	276/840

TABLE 2 Results from fits of simple power-law + Galactic absorption models to the *Chandra* image-spectra of RX J1131-1231.

Optical and X-ray monitoring of microlensing events in AGN

The brightness of the images in RXJ 1131-1231 will vary for two main reasons:

(a) Intrinsic variability of the quasar will appear shifted in time in each of the lensed images due to the different light travel times associated with each image. The time delays between images are (from Morgan et al. 2006) :

A-B = 12.0 (-1.3,+1.5) days
A-C = 9.6 (-1.6,+2.0) days
A-D = -87 +/- 8 days.

(b) Microlensing by stars in the lensing galaxy will produce uncorrelated variability between images. The strength of this variability will in part depend on the relative size of the source to the Einstein radius size ζ_E.

Optical and X-ray monitoring of microlensing events in AGN

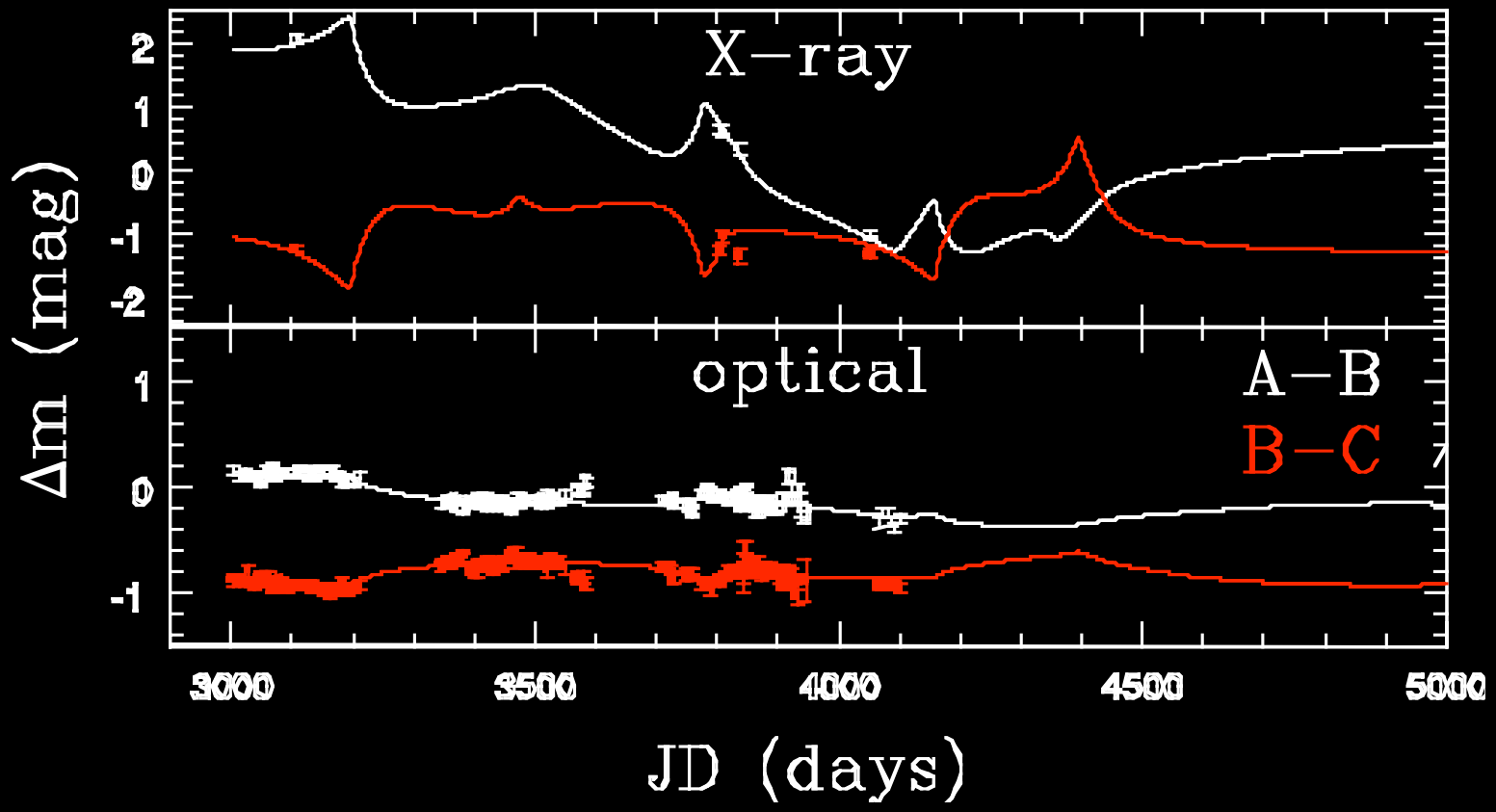

We show the X-ray and optical flux ratios between the images of RX J1131-1231.

Optical and X-ray monitoring of microlensing events in AGN

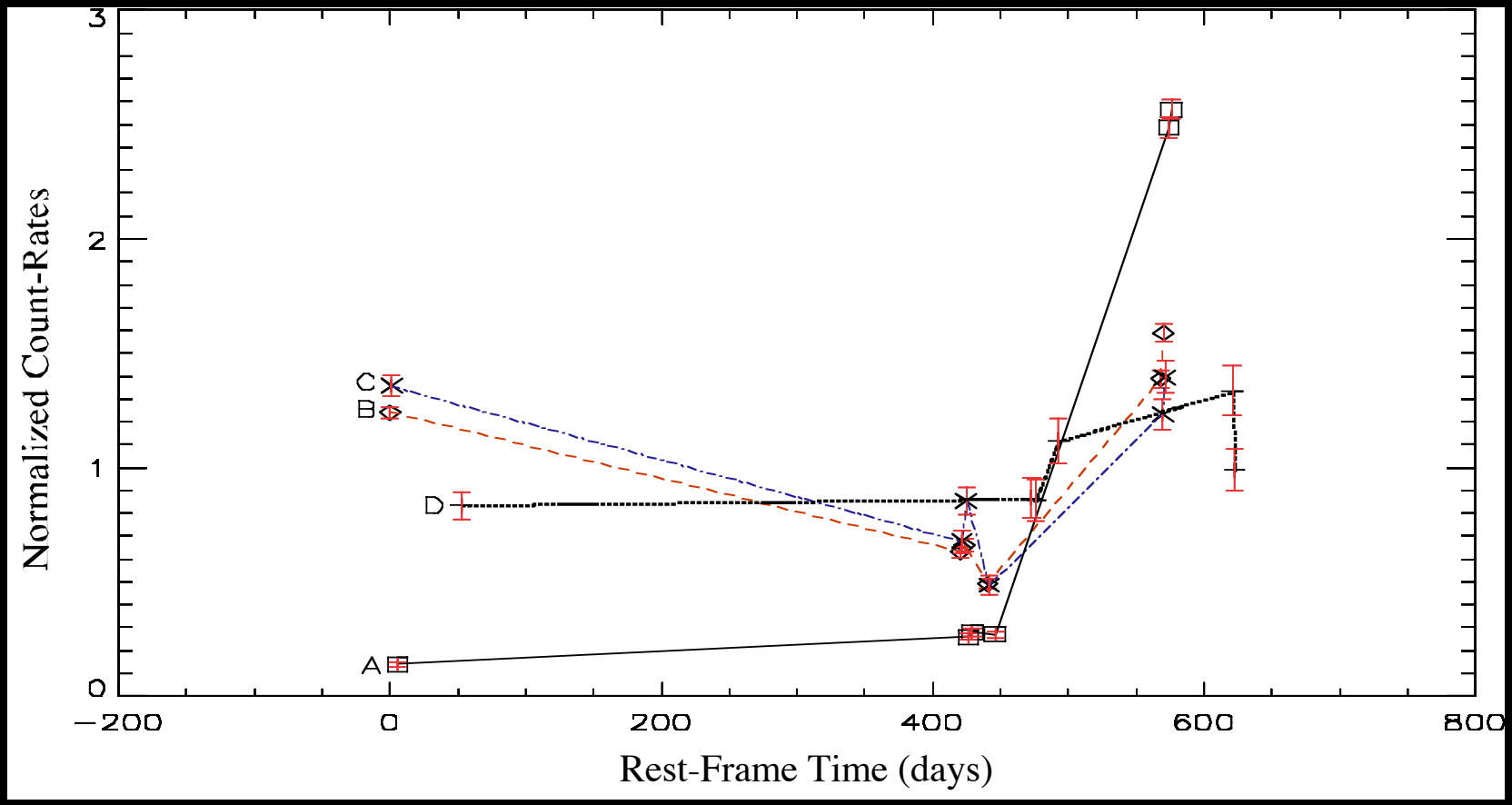

Light curve in the rest-frame of RX J1131-1231. The count-rate of each image is normalized to the mean count-rate of the image for the six observations.

Optical and X-ray monitoring of microlensing events in AGN

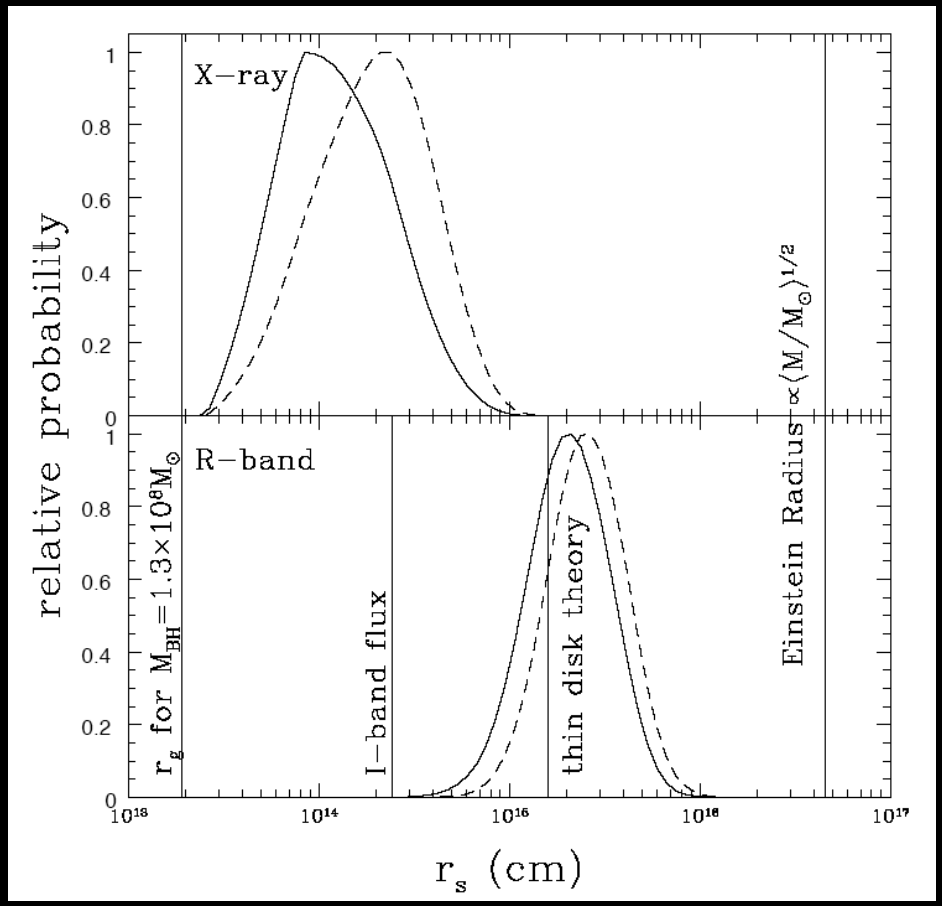

The probability distributions for the size of the X-ray (top) and R-band (400 nm in the rest frame) optical (bottom) emission regions for the log (solid) and linear (dashed) size priors. The vertical lines mark the gravitational radius rg for a RXJ1131 black hole, the Einstein radius for <M> = M_{solar} and the accretion disk size estimates based on either the I-band flux or thin disk theory.

Clusters of galaxies in the vicinity of Q1131-1231

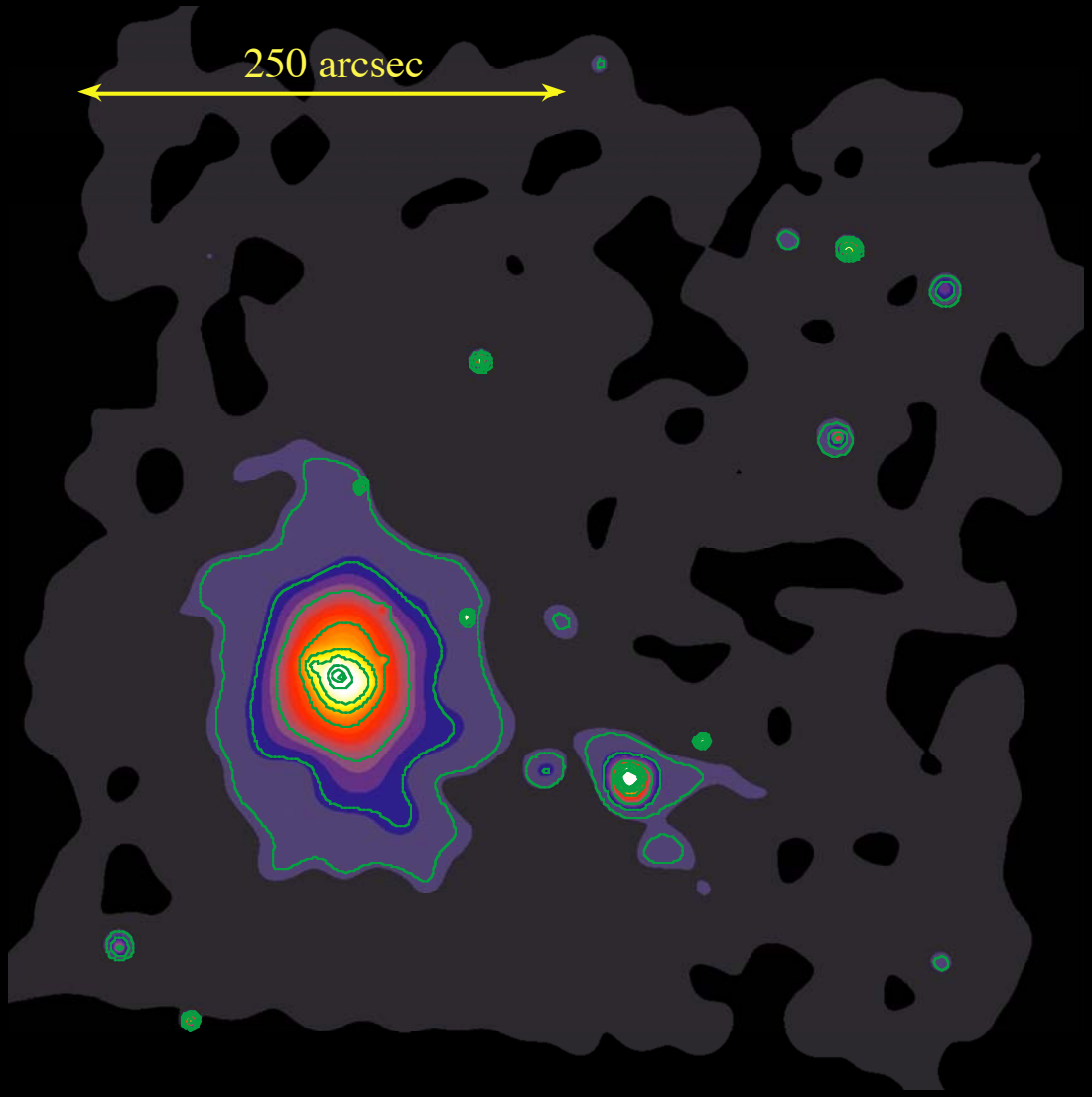

Spatial Analysis

Model : 2D-β + background

Results :
β = 0.4 +/- 0.2
r_0 = 4.2 +/- 0.3 arcsec
ε= 0.10 +/- 0.03

Spectral Analysis

Model : wabs*mekal

Results :
T_e = 1.3 +/- 0.08 keV
A = 0.6 +/- 0.3
z = 0.1
L(2 - 10 keV) = 3 x 10^{43} erg/s

(consistent with Morgan et al. 2006)

Clusters of galaxies in the vicinity of Q1131-1231

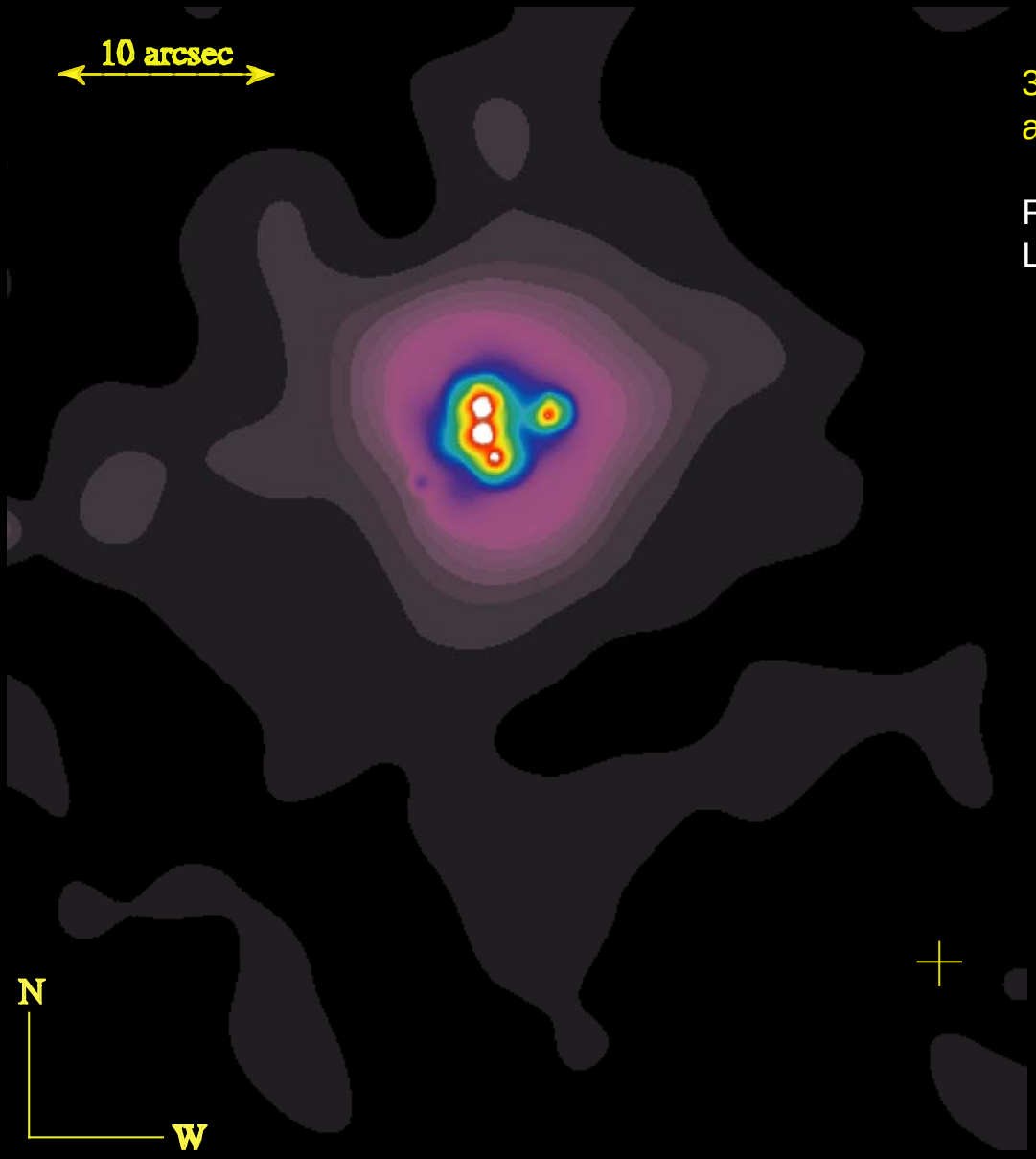

3 σ upper limits on possible cluster at z = 0.295 located at cross.

F(2 - 10 keV) = 6 x 10^{-15} erg s^{-1} cm^{-2}
L(2 - 10 keV) = 2.6 x 10^{42} erg s^{-1}

CONCLUSIONS

1. X-ray monitoring observations of RX J1131-1231 show significant uncorrelated variability between images. This is strong evidence for the presence of microlensing in this system. The significant tenfold rise in the X-ray flux of image A during the last two observation epochs is most likely caused by a microlensing event.

2. Modeling of the X-ray and optical light curves of RX J1131-1231 indicates that the X-ray and optical emission regions have sizes of 6 r_g and 100 r_g, respectively.. Additional X-ray and optical observations will confirm these results and reduce the uncertainties (factors of 2 and 1.6, respectively) in these estimates.